Review

Challenges and modification strategies of air-processed all-inorganic CsPbX₃ perovskite films for efficient photovoltaics

Li Cao[1,#] (ID), **Yu Tong**[2,3,#] (ID), **Hongqiang Wang**[2,3] (ID), **Kun Wang**[1,3,*] (ID)

[1]School of Microelectronics, Northwestern Polytechnical University, Xi'an 710072, Shaanxi, China.
[2]State Key Laboratory of Solidification Processing, Center for Nano Energy Materials, School of Materials Science and Engineering, Northwestern Polytechnical University, Xi'an 710072, Shaanxi, China.
[3]Chongqing Innovation Center, Northwestern Polytechnical University, Chongqing 401135, China.
[#]Authors contributed equally.

*Correspondence to:** Prof. Kun Wang, School of Microelectronics, Northwestern Polytechnical University, 127 West Youyi Road, Beilin District, Xi'an 710072, Shaanxi, China. E-mail: kunwang@nwpu.edu.cn

Abstract

All-inorganic perovskites CsPbX₃ (X: halogen ions) have gained significant attention for application in next generation photovoltaic technologies due to their superior thermal stability and excellent optoelectronic properties. Compared with fabrication in N_2 glove boxes, ambient air processing could simplify the operation and reduce the fabrication cost, which is favorable for boosting the commercialization of perovskite solar cells (PSCs). However, the moisture in ambient air tends to cause the phase transformation of inorganic perovskite from the photoactive black phase to the photo-inactive yellow one, thus deteriorating the photovoltaic performance. Considering the obstacles from both the intrinsic structure instability and the external atmosphere, tremendous efforts have been made for pursuing high-efficiency and stable all-inorganic PSCs that can be processed in ambient air. In this review, we first analyze the challenges for fabricating CsPbX₃ in ambient air from both the intrinsic characters and external atmosphere and then overview the progress of the air-fabricated CsPbX₃ films for photovoltaic applications. The recently reported various modification strategies, including the compositional/precursor, solvent, additive, and interface engineering, for achieving high-quality and stable CsPbX₃ films are comprehensively summarized. Finally, a brief conclusion and outlook is given to inspire more research interest on air-fabricated CsPbX₃ photovoltaics. This review provides significant guidance for further optimizing the air-processible CsPbX₃ films to boost the large-scale commercialization of cost-effective PSCs in the future.

Keywords: All-inorganic perovskite solar cells, ambient fabrication, efficiency, stability

INTRODUCTION

Metal halide perovskites have garnered great attention for application in the photovoltaic field owing to their high absorption coefficient, low exciton binding energy and long carrier lifetime[1]. Recently, a high record power conversion efficiency (PCE) of over 26% has been achieved for the perovskite solar cells (PSCs)[2], which makes them competitive with conventional crystalline silicon solar cells. Nevertheless, the organic parts in the metal halide perovskites generally show the disadvantages of easy volatilization under high temperatures (over 200 °C), severely restricting the long-term operational and thermal stability of PSCs[3,4]. In contrast, the all-inorganic $CsPbX_3$ (X: halogen ions) perovskite materials, with the inorganic cesium ions (Cs^+) completely replacing the A-site organic ions, exhibit better thermal and light stability, rendering them suitable for practical applications[5-7]. In 2015, Eperon *et al.* first reported all-inorganic $CsPbX_3$ PSCs with a PCE of 2.9%[8]. Soon after, more stable $CsPbI_3$ perovskite quantum dot (QD) solar cells were developed, with an open-circuit voltage (V_{OC}) of 1.23 V and a PCE over 10%[9]. Recently, Wang *et al.* developed a defect passivation strategy for $CsPbI_3$ films and prepared PSCs with a PCE of 21.8%, which is a record efficiency for the all-inorganic $CsPbX_3$ PSCs so far[10]. Although all-inorganic PSCs have presented great progress in the past years, their fabrication under inert atmosphere in a glove box hinders future large-scale production. By contrast, fabricating PSCs in ambient air is drawing more and more attention because of their easy operation and low fabrication cost[11]. However, the intrinsic structural instability and the degradation induced by the external environment remain huge challenges for fabricating high-quality $CsPbX_3$ perovskite films in ambient conditions.

The quality of photoactive perovskite layers, including uniformity, crystallinity, surface roughness, defect density, structure stability, *etc.*, which influence the carrier transport and recombination kinetics, determines the photovoltaic performance of the PSCs. To stabilize the crystal structure and raise the quality of air-processed $CsPbX_3$ perovskite films, many strategies have been reported, such as crystallization regulation, composition or precursor engineering, surface modification with highly hydrophobic groups, *etc.* With these modifications, significant achievements in PCE have been realized in recent years. The efficiency evolution of air-processed all-inorganic PSCs is shown in Figure 1A. Therefore, it is meaningful to summarize the conducive strategies for improving the quality of air-processed all-inorganic perovskites in PSCs. Herein, we mainly focus on the challenges of all-inorganic PSCs fabricated in an ambient atmosphere and the most recently developed modification strategies. First, the instability issues are discussed from both the intrinsic characteristics and extrinsic atmosphere aspects. Subsequently, we summarize the modification strategies from composition and precursor, solvent, additive introduction, and interface engineering [Figure 1B]. Finally, a brief conclusion and outlook is given.

INSTABILITY ORIGIN

Although tremendous research has been conducted and significantly improved performance has been achieved on $CsPbX_3$ PCSs, most devices are fabricated in glove boxes with strictly controlled low moisture and oxygen content owing to the intrinsic instability and the accelerated degradation process induced by air atmosphere. Understanding the influence factors and the underlying mechanisms for the instability of perovskites is necessary to obtain high-quality perovskite films and good-performance PSCs under ambient air. This section summarizes the potential factors contributing to the instability from intrinsic characteristics and external conditions in ambient air.

Intrinsic characteristics

The ideal three-dimensional (3D) $CsPbX_3$ crystal structure is a cubic phase with an octahedron structure[5]. As shown in Figure 2A, the cation Pb^{2+} is located at the center of a regular octahedron of anion X^-, and the
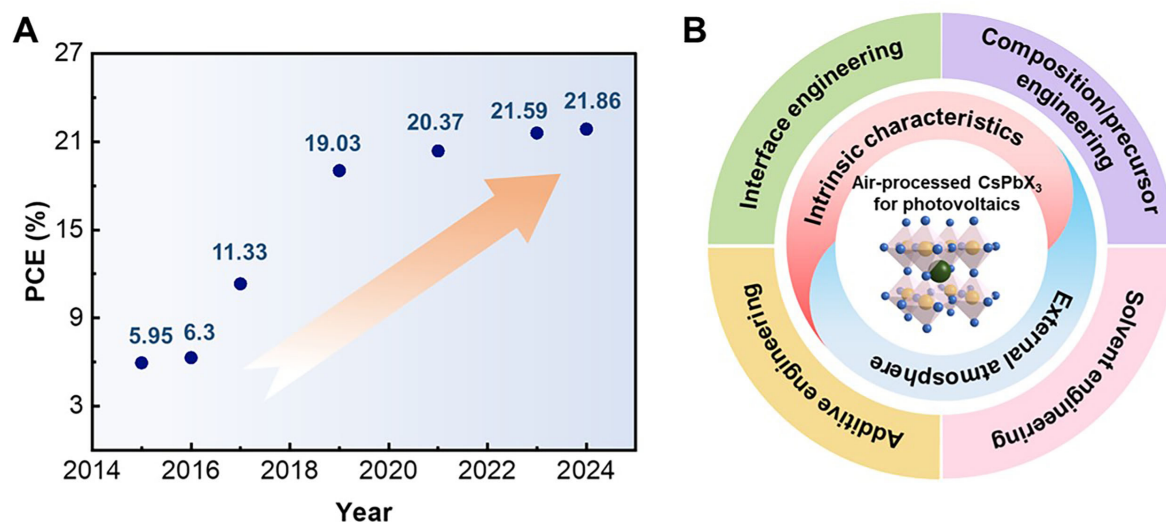
Figure 1. (A) PCE evolution of air-processed all-inorganic PSCs. (B) Illustration of modification strategies for air-processed all-inorganic PSCs.
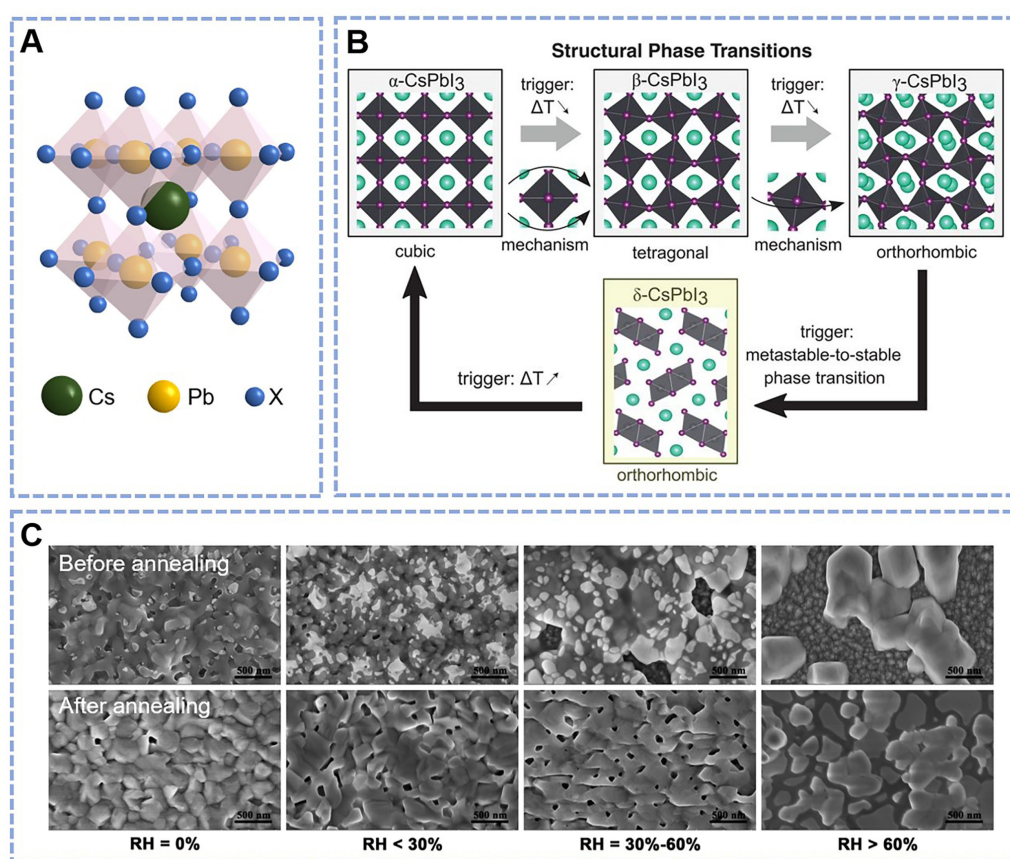
Figure 2. (A) Schemes of the 3D cubic $CsPbX_3$ perovskite structure. (B) Crystal structure of $CsPbI_3$ perovskite with different phases and their relative phase transitions. Copyright from Ref[13]. (C) Morphologies of $CsPbI_3$ films prepared under different RH conditions before and after annealing. Copyright from Ref[20].

inorganic cation Cs^+ is surrounded by eight lead halide $[PbI_6]^{4-}$ octahedra. Under this circumstance, the crystal structure of $CsPbX_3$ presents a highly symmetrical feature. However, owing to the small radius of Cs cation, the Goldschmidt tolerance factor t of $CsPbX_3$ is lower than the organic-inorganic counterparts as *t* can be determined by

$$t = \frac{(r_A + r_X)}{\sqrt{2}(r_B + r_X)} \tag{1}$$

where r_A, r_B, and r_X are the ionic radii for cation A, cation B, and anion X, respectively[12]. As a result, the lead iodide octahedra is prone to distort and the corner-sharing $[PbI_6]^{4-}$ octahedra tends to rotate, lowering its symmetry. For example, three types of photoactive black crystal polymorphs are reported for $CsPbI_3$ along decreasing the temperature: the cubic (α-, Pm3m), tetragonal (β-, P4/mbm), and orthogonal black phases (γ-, Pbnm), following a tendency of decreased symmetry [Figure 2B][13]. Moreover, the black phases prefer to further distort and degrade into the photo-inactive yellow phase (δ-, Pnma), owing to the lowest formation energy. This explains the phase instability of $CsPbI_3$. The phase transition greatly influences the optoelectronic properties, including the density of states, electronic band structure, exciton binding energy, *etc.* Substituting the I ion with smaller Br or Cl ions would increase the *t* value, thus enhancing the structure stability of all-inorganic perovskites. However, other problems, such as widened bandgap for reduced photo absorption, difficulty dissolving in commonly used solvents, *etc.*, may appear. Therefore, the reported all-inorganic PSCs with high performance mostly rely on $CsPbI_3$ or $CsPbI_3$ with a small amount of Br substitution.

Apart from the phase instability, ion migration would destroy the perovskite lattice and degrade the optoelectronic properties. As ionic materials with low formation energies and migration activation energies, the triggered tremendous vacancies provide pathways for ion migration to the adjacent contact layers, and this process more easily occurs under heat and light. It was reported that vacancy-assisted ion migration is one of the most common processes owing to the low defect formation energy in $CsPbI_3$[14]. Such induced iodine vacancy defects may not aggravate the non-radiative recombination as shallow-level defects are mainly formed in this case. However, it will speed up the decomposition rate of the perovskite structure. Apart from the vacancy-assisted ion migration, the grain boundaries formed during fabrication may also facilitate the ion migration of the perovskite films compared to the interior of the grains[15,16]. Therefore, decreasing the number of grain boundaries is also considered an effective way to mitigate the ion migration. Although a "self-healing" process was reported to partially suppress the ion migration[17], the device's photovoltaic performances, especially the hysteresis and long-term stability, are still far from satisfactory.

External atmosphere

Although the stability of $CsPbX_3$ perovskite films depends on the intrinsic characteristics, the external atmosphere, such as humid air, can accelerate the degeneration process. To develop complete air processing strategies for all-inorganic PSCs, the role of the environmental atmosphere for manufacturing $CsPbX_3$ perovskite films should be highlighted. In this section, the instability caused by environmental factors, including water and oxygen, is discussed.

Impact of water

It is well known that water generally causes the degradation of organic-inorganic halide perovskites, which brings problems to preparing and storing PSCs[18]. Water molecules can be easily absorbed at the vacancy sites at the surface and grain boundaries of the perovskite films[19]. In a humid environment, water molecules lower the free-energy barrier of the phase transitions and the inevitable defects in the prepared
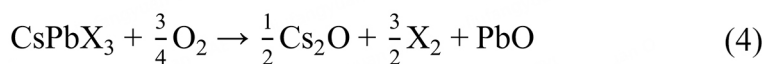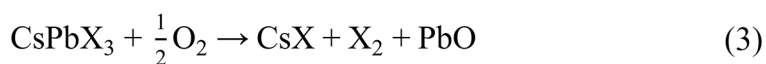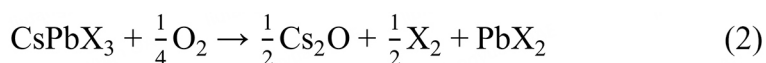
CsPbX$_3$ PSCs provide pathways for water invasion[19]. In those situations, water molecules adsorbed on CsPbX$_3$ perovskite film would trigger the phase transition from α-phase to δ-phase and accelerate the degradation of perovskites in a humid environment.

In addition, the water molecules probably have a non-negligible influence on the crystalline structure and morphology of the CsPbX$_3$ films during a series of thermodynamic and kinetic processes. It has been pointed out that a high humidity environment tends to result in CsPbI$_3$ perovskite films with poor quality. Liang *et al.* contrasted the morphologies of the CsPbI$_3$ films fabricated under different humidity conditions [Figure 2C][20]. Without annealing, the spin-coated CsPbI$_3$ films present remarkably different morphologies at varying relative humidity (RH). Decreasing surface coverage and increasing number of cavities are observed with rising RH. When RH exceeds 60%, the CsPbI$_3$ films presented low surface coverage, large crystal islands, and large gaps. After annealing, more compact films can be obtained. However, upon increasing RH, more holes and even cracks present in CsPbI$_3$ films, with the crystal grains obviously separating from each other under high humidity conditions (RH > 60%), which might be attributed to the corrosion caused by excessively high humidity. For the PSCs with traditional regular n-i-p structure, dopants with strong hygroscopicity are usually used in 2,2′,7,7′-tetrakis- (N,N-di-4-methoxyphenylamino)-9,9′-spirobifluorene (spiro-MeOTAD), which might pose an additional threat to the stability of all-inorganic perovskite in moist air[21,22].

The above experimental results demonstrate the detrimental effect of moisture on CsPbI$_3$ perovskite films. However, an extremely low humidity environment is not a prerequisite for preparing all-inorganic perovskite films. Interestingly, some research even indicates that an appropriate amount of water could control the crystallization of all-inorganic perovskites for improving the photovoltaic performance[23].

Impact of oxygen
When processing in an open environment, oxygen would be unavoidable so its impact needs to be considered. For organic-inorganic hybrid perovskite, the degradation caused by oxygen has been reported, which involves both the deprotonation of the organic cation and the breaking of the local Pb-I octahedral structure via forming O-Pb bonds[24,25]. In contrast, for CsPbI$_3$ with no organic components, the deprotonation of the organic components could be avoided. Tsvetkov *et al.* reported that the stability of inorganic perovskite can be influenced by the presence of gaseous O$_2$, and the possible degradation pathways are as follows[26]:

$$CsPbX_3 + \frac{1}{4}O_2 \rightarrow \frac{1}{2}Cs_2O + \frac{1}{2}X_2 + PbX_2 \qquad (2)$$

$$CsPbX_3 + \frac{1}{2}O_2 \rightarrow CsX + X_2 + PbO \qquad (3)$$

$$CsPbX_3 + \frac{3}{4}O_2 \rightarrow \frac{1}{2}Cs_2O + \frac{3}{2}X_2 + PbO \qquad (4)$$

This work also indicated that CsPbI$_3$ is more sensitive to O$_2$ and may undergo more severe degradation in the presence of O$_2$ than CsPbCl$_3$ and CsPbBr$_3$. However, unlike water whose effects on all-inorganic perovskites have been widely explored, very limited reports are on the impact of oxygen[26,27]. Further studies on how oxygen influences inorganic perovskites and the underlying mechanisms still need to be investigated.

MODIFICATION STRATEGIES

Based on the above discussion, we conclude that the challenges of fabricating $CsPbX_3$ in ambient air mainly stem from the intrinsic instability and moisture-assisted degradation. Therefore, to improve the perovskite film quality, most strategies focus on modulating the material itself and protecting the inorganic perovskite films against moisture invasion. Table 1 lists inorganic PSCs fabricated in air. This section comprehensively summarizes the recently reported effective modification strategies.

Composition/precursor engineering

Increasing the tolerance factor of $CsPbI_3$ by doping with other ions, e.g., a larger A-site cation, a smaller B-site cation, or a smaller X-site cation, has been reported as an effective method to enhance the stability. For example, Sn and Ge, the same group elements with Pb, have been incorporated into the perovskite lattice to improve the phase stability of all-inorganic perovskites fabricated in ambient air[28,30]. Besides, lanthanide elements, such as Eu^{3+}, La^{3+}, Yb^{2+}, Ho^{3+}, *etc.*, are also introduced to regulate the crystal structure and help improve the phase stability of $CsPbX_3$ perovskite, therefore enhancing the PCE of devices[33-36]. Jena *et al.* prepared α-$CsPbI_3$ films at a lower annealing temperature (85 °C) by incorporating Eu^{3+} into perovskite[29]. After optimization, the $CsPbI_3$ perovskite films could maintain α-phase stability for more than 30 days under ambient air. Mali *et al.* employed a dual bulk and surface passivation strategy with $CsPb_{1-x}Tb_xI_2Br$ QDs to stabilize the photoactive γ-phase $CsPb_{1-x}Tb_xI_2Br$ absorber in ambient air [Figure 3A], thereby promoting the PCE to 17.51% with negligible hysteresis and significantly enhanced operational stability, and further to 19.01% for γ-$CsPb_{0.95}Tb_{0.05}I_{2.5}Br_{0.5}$-based devices[63]. Additionally, Ba^{2+}, In^{3+}, and Cd^{2+} cations are also used to partially substitute Pb^{2+} for stabilizing black-phase $CsPbI_2Br$ in ambient conditions[22,31]. For example, In cation is introduced into the $CsPbI_2Br$ crystal for fabricating pinhole-free perovskite films with improved stability under ambient conditions, thus obtaining a record efficiency for the devices with dopant-free hole transport layer at that time and > 95% retaining of the PCE after 1,600 h of operation[22]. Moreover, it was reported that smooth and compact Cd-doped $CsPbI_{2.5}Br_{0.5}$ perovskite thin films can be obtained on a spray-deposited electron transport layer under ambient air[22]. The optimized devices show a PCE of up to 19.75% and a stable performance in the air for more than 300 h.

For the A-site incorporation, it is difficult to seek an inorganic cation for substituting or partially substituting Cs^+ due to its largest radius among the monovalent metals. However, Patil *et al.* found that Rb incorporation at the A-site helps obtain high-quality $CsPbI_2Br$ perovskite thin films with high compactness, uniform and pinhole-free morphology together with improved thermal stability, revealing that partial incorporation with Rb^+ cation can stabilize black phase all-inorganic perovskites under ambient conditions[32].

Apart from the cation engineering, reasonable incorporation of relatively smaller anions in the X-site of the $CsPbX_3$ perovskite material can also improve the structure stability. Substitution of I with Br is a mostly reported approach to increase the tolerance factor and improve the phase stability when processing in ambient air. However, the subsequently increased bandgap of the material is inevitably induced, resulting in lower light harvesting. Hence, adjusting the amount of Br doping and looking for more appropriate anions to balance the stability and the bandgap is of significant importance.

Precursor engineering is also a facile strategy for fabricating stable all-inorganic PSCs under ambient conditions. In earlier studies, the commonly used precursor solutions contain CsI and PbI_2 for fabricating $CsPbI_3$. Xiang *et al.* proposed a strategy to prepare air-stable α-$CsPbI_3$ PSCs using $HPbI_3$ to replace PbI_2[37]. In 2020, Duan *et al.* proposed a new precursor system (HCOOCs, $HPbI_3$, and $HPbBr_3$) to prepare ambient-compatible, high-efficient and stable $CsPbI_2Br$ PSCs under high-humidity conditions (91% RH) [Figure 3B][38]. In this precursor system, a new complex (HCOOH•Cs^+) is formed, which is crucial for

Table 1. Summary of all-inorganic PSCs fabricated in air

Device structure	V_{oc}[V]	J_{sc}[mA cm^{-2}]	FF [%]	PCE [%]	Fabrication condition	Ref.
Compositional engineering						
FTO/c-TiO$_2$/m-TiO$_2$/CsPb$_{0.9}$Sn$_{0.1}$IBr$_2$/carbon	1.26	14.3	63	11.33	RH 90%	[28]
FTO/TiO$_2$/CsPbI$_3$/spiro-OMeTAD/Au	0.898	11.1	68	6.8	RH: 0%-20%	[29]
FTO/SnO$_2$/CsPb$_{0.8}$Ge$_{0.2}$I$_2$Br/P3HT/spiro-OMeTAD/Au	1.27	12.15	70.1	10.8	RH: -	[30]
FTO/c-TiO$_2$/m-TiO$_2$/BaI$_2$: CsPbI$_2$Br/P3HT/Au	1.21	15.45	79.45	14.85	RH: -	[31]
FTO/c-TiO$_2$/m-TiO$_2$/Cs$_{0.99}$Rb$_{0.01}$PbI$_2$Br/P3HT/Au	1.32	16.25	80.03	17.16	RH: 20%-30%	[32]
FTO/c-TiO$_2$/m-TiO$_2$/CsPb$_{0.98}$La$_{0.02}$I$_2$Br/carbon	1.12	11.66	61.24	8.03	RH: 20%-30%	[33]
FTO/c-TiO$_2$/m-TiO$_2$/CsPb$_{0.97}$Yb$_{0.03}$I$_2$Br /P3HT/Au	1.267	15.94	76.35	15.41	RH: -	[34]
FTO/c-TiO$_2$/m-TiO$_2$/InCl$_3$:CsPbI$_2$Br/P3HT/Au	1.334	16.34	80.1	17.45	RH: -	[35]
FTO/TiO$_2$/InCl$_3$:CsPbI$_2$Br/P3HT/Au	1.303	15.9	75.76	15.69	RH: -	[22]
FTO/c-TiO$_2$/m-TiO$_2$/CsPbI$_{2.5}$Br$_{0.5}$/P3HT/Au	1.272	19.5	79	19.59	RH: -	[36]
Precursor engineering						
FTO/TiO$_2$/CsPbI$_3$/carbon	0.79	18.5	65	9.5	RH: 10%-20%	[37]
FTO/TiO$_2$/CsPbI$_2$Br /PTAA/Au	1.32	15.34	79.54	16.14	RH: -	[38]
ITO/SnO$_2$/LiF/CsPbI$_2$Br/PPAI/ spiro-OMeTAD/MoO$_3$/Ag	1.33	16.14	79.45	17.01	RH: 25%-65%	[39]
Solvent and anti-solvent engineering						
FTO/SnO$_2$/CsPbI$_2$Br/spiro-OMeTAD/MoO$_3$/Ag	1.30	17.67	74.18	17.10	RH: 20%-70%	[40]
ITO/PEDOT:PSS/CsPbI$_3$/ PCBM/Al	1.05	18.66	73.3	14.4	RH: -	[41]
FTO/TiO$_2$/CsPbI$_3$/PTAA/Au	1.11	18.31	77.97	15.91	RH: -	[20]
FTO/TiO$_2$/CsPbI$_3$/Spiro-OMeTAD/Au	1.18	20.17	80.55	19.17	RH: 60%	[42]
Additive engineering						
FTO/c-TiO$_2$/CsPbI$_3$/spiro-OMeTAD/Ag	0.66	11.92	52.47	4.13	RH < 30%	[43]
FTO/TiO$_2$/CsPbI$_3$/spiro-OMeTAD/Ag	1.137	20.23	82.7	19.03	RH: 5%-10% (dry box)	[44]
FTO/SnO$_2$/CsPbI$_3$/spiro-OMeTAD/Au	1.1	20.21	80.94	19	RH: ~35%	[45]
ITO/P3CT-N/CsPbI$_3$/ PCBM/C$_{60}$/BCP/Ag	1.16	20.46	81.13	19.25	RH: 40%	[46]
ITO/P3CT-N/CsPbI$_3$/ PCBM/C$_{60}$/BCP/Ag	1.176	20.1	80.04	18.93	RH: 40%	[47]
FTO/TiO$_2$/CsPbI$_2$Br/spiro-MeOTAD/Au	1.28	16.56	81.64	17.26	RH: -	[48]
ITO/P3CT-N/CsPbI$_3$/ PCBM/C$_{60}$/BCP/Ag	1.225	20.33	77.37	19.27	RH: ~35%	[49]
FTO/TiO$_2$/CsPbI$_2$Br/carbon	1.25	14.47	80.1	14.49	RH: 30%-70%	[50]
ITO/P3CT-N/CsPbI$_3$/ PCBM/C$_{60}$/TPBi/Cu	1.172	20.58	78.84	19.01	RH: 40%-80%	[51]
FTO/TiO$_2$/CsPbI$_3$/ spiro-OMeTAD/Au	1.244	20.60	82.52	21.15	annealing in air (RH: -)	[52]
FTO/TiO$_2$/SnO$_2$/β-CsPbI$_3$/γ-CsPbI$_3$/P3HT/Au	1.22	21.72	81.5	21.59	β-CsPbI$_3$ prepared in air (RH: 25%-30%)	[53]
FTO/TiO$_2$/CsPbI$_3$/P3HT/Au	1.16	20.99	83.1	20.25	RH: -	[21]
Interface engineering						
FTO/ZnO-ZnS/m-TiO$_2$/CsPbI$_3$/spiro-MeTAD/Au	1.06	20.56	77.61	16.91	RH: 10%-15% (dry box)	[54]
FTO/TiO$_2$/CsPbI$_3$/MACl/ spiro-OMeTAD/Au	1.198	20.59	82.5	20.37	RH: 15%-30%	[55]
ITO/P3CT-N/CsPbI$_3$/ PCBM/C$_{60}$/BCP/Ag	1.213	20.44	80.37	19.84	RH 40%	[56]
ITO/PEDOT:PSS/CsPbI$_3$/PCBM/BCP/Ag	1.02	19.12	79.18	15.45	RH 30%	[57]
ITO/P3CT-N/CsPbI$_3$/ PCBM/C60/TPBi/Ag	1.18	20.84	81.90	20.18	RH: 20%-40%	[58]
FTO/TiO$_2$/DCB/CsPbI$_3$/	1.26	20.71	83.8	21.86	RH: 30%	[59]

spiro-OMeTAD/Ag						
Combined engineering						
FTO/TiO$_2$/CsPbI$_3$/spiro-OMeTAD/Ag	1.11	20.23	82	18.4	RH: < 10%	[60]
ITO/PEDOT:PSS/CsPbI$_3$/PCBM/BCP/Al	0.95	19.39	71.57	13.21	RH: < 55%	[61]
FTO/TiO$_2$/CsPbI$_3$/spiro-OMeTAD/Au	1.15	19.43	84.33	18.84	RH: 30%-40%	[62]
FTO/c-TiO$_2$/m-TiO$_2$/CsPb$_{0.9}$Tb$_{0.05}$I$_{2.5}$Br$_{0.5}$/P3HT/Au	1.315	16.34	81.53	17.51	RH: -	[63]
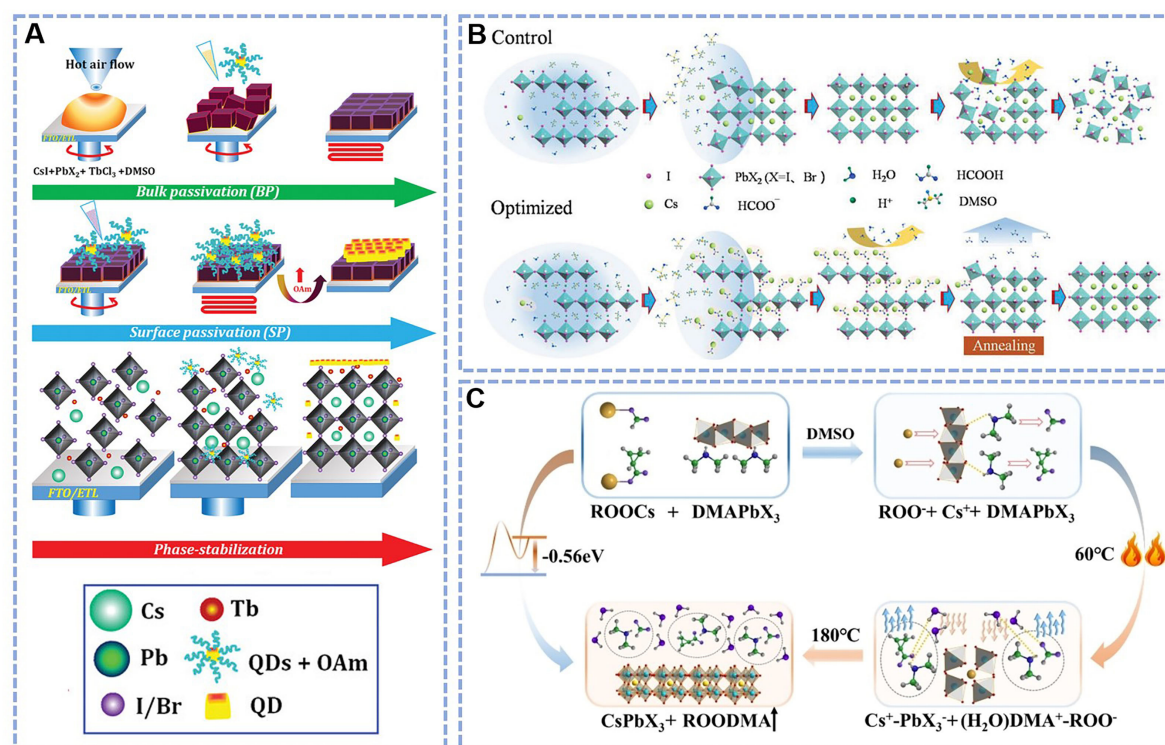
Figure 3. (A) Schematic illustration of nucleation and crystal growth procedures of CsPb$_{1-x}$Tb$_x$I$_2$Br perovskite films and passivation by γ-CsPb$_{1-x}$Tb$_x$I$_2$Br QDs. Copyright from Ref[63]. (B) Schematics of the crystallization processes of the control and optimized perovskite with precursors of HCOOCs and HPbX$_3$. Copyright from Ref[38]. (C) Schematically illustrated formation process of CsPbI$_2$Br with Cs-acid and DMAPbX$_3$ as precursor Copyright from Ref[39].

controlling the crystallization process, leading to compact and uniform CsPbI$_2$Br films with larger grain sizes. Recently, Yue *et al.* used Cs acid and DMAPbX$_3$ (DMA: dimethylammonium) as a precursor to assemble the CsPbI$_2$Br crystals [Figure 3C][39]. In this case, the evaporation enthalpy of the DMA-acid side product is modified, making the CsPbI$_2$Br perovskites insensitive to environment humidity. Therefore, PSCs with a PCE exceeding 17% have been achieved, with enhanced shelf storage and 85/85 (temperature/ humidity) tests.

Solvent engineering

For fabricating inorganic PSCs, the most generally employed solvents are N,N-dimethylformamide (DMF) and dimethyl sulfoxide (DMSO) owing to the dissolvability of lead halides and cesium halides in other popular solvents[40]. Apart from the single DMF or DMSO solvent[31,35,64], mixed solvents of DMF and DMSO are also used, and the ratio between them has been adjusted to enhance the device performance[65,66]. In more recent work, methylammonium acetate (MAAc) was reported to be an excellent and eco-friendly solvent for CsPbX$_3$ precursor solution in one-step humidity-insensitive fabrication[40,41]. The coordination

interaction plays an important role in perovskite crystallization. In the MAAc system, the interaction is stronger than in the DMF:DMSO system due to strong N-H···I hydrogen bonds and Pb-O bonds. Wang *et al.* reported ambient processed $CsPbI_{2.5}Br_{0.5}$ PSCs using MAAc as a solvent, achieving a PCE of 17.10 % and V_{OC} of 1.30 V [Figure 4A][40].

Owing to high boiling point of the frequently used DMF and DMSO solvents, the slow evaporation of solvent would readily cause the slow nucleation rate. It has been indicated that anti-solvents, including the widely employed chlorobenzene (CB), ethyl acetate (EA), *etc.*, rapidly reduce the solubility of the precursor and accelerate the nucleation[67]. Adjusting the operation of anti-solvents during the spin-coating process of perovskite films can mediate the nucleation and grain growth of the perovskite films, thus modifying the morphology, film coverage and defect density[68,69]. Liang *et al.* conducted an anti-solvent hot substrate spin-coating method to construct air-fabricated $CsPbI_3$ PSCs, realizing good optoelectronic properties similar to the N_2-fabricated devices and a PCE of 15.91%[20]. Jeong *et al.* proposed an anisole antisolvent bathing strategy for preparing DMAI-assisted $CsPbI_3$ films [Figure 4B][62]. During this process, rapid crystallization kinetics can be attributed to the formation of the Cs_4PbI_6-antisolvent adduct which lowers the transformation energy barrier, therefore resulting in a more uniform film with better coverage, fewer defects and pinholes. The obtained devices show a PCE of 18.84% under moisture processing conditions (30%-40% RH). Wang *et al.* used methyl acetate as an anti-solvent and introduced perhydropolysilazane (PHPS) into this anti-solvent to develop a curing-anti-solvent strategy for fabricating black-phase $CsPbI_3$ perovskite films under ambient conditions [Figure 4C][42]. Under humid conditions, the hydrolyzed products of PHPS can adjust the grain growth by forming Lewis acid-base adducts. The pyrolysis-generated Si-O-Pb bonding to $CsPbI_3$ grains can create a shield layer to hinder phase transition. The resulting PSCs show a remarkably improved PCE of 19.17%, even at RH 60%.

Additive engineering

Introducing additives into the perovskite precursor solutions can influence perovskite crystallization and film formation, passivate the defects, and tune the structure and energetics, either in N_2 atmosphere or ambient air[70,71]. This section overviews the recent progress in additive engineering to improve the air-processed all-inorganic perovskite film quality and device performance.

Luo *et al.* first fabricated $CsPbI_3$ PSCs under fully open-air conditions by adding HI, which improves the solubility of CsI and PbI_2 precursors in DMF solution and helps $CsPbI_3$ transform from the yellow non-perovskite to the black perovskite under low temperature[43]. After that, various additives are used to improve the air-processed film quality and the resultant effects on the PCE of devices have also been deeply investigated. DMAI is one of the most widely used additives for fabricating stable $CsPbX_3$ and introducing HI and $HPbI_3$ routes share the same mechanism due to the generated DMA through the reaction of HI with DMF[44,51,60,62]. Wang *et al.* investigated the role of DMAI in $CsPbI_3$ perovskite films fabricated in a dry box with an accurately controlled humidity (5%~10% RH), which indicated that DMAI is a volatile additive to control the crystalline perovskite, rather than alloying into the crystal lattice of $CsPbI_3$ perovskite [Figure 5A][44]. Besides, they stated that the DMAI residues in perovskite film can deteriorate the device performance. Together with phenyltrimethylammonium chloride (PTACl) passivation, the photovoltaic device exhibits a high efficiency of 19.03 %. Recently, Li *et al.* developed a hydrogen-bonding-facilitated DMA extraction strategy to prepare γ-$CsPbI_3$ films [Figure 5B][21]. With the formation of hydrogen bonds between polyacrylic acid (PAA) and DMA cation, the escape energy barrier of DMA is reduced, accelerating the decomposition of $DMAPbI_3$ and the crystallization kinetics of $CsPbI_3$. Therefore, pinhole-free $CsPbI_3$ films can be obtained without any trace of $DMAPbI_3$ residue and the fabrication humidity can be extended up to 80%. Consequently, dopant-free poly(3-hexylthiophene) (P3HT)-based photovoltaic devices with an outstanding PCE of 20.25% and superior moisture and operational stability can be achieved. Meanwhile,
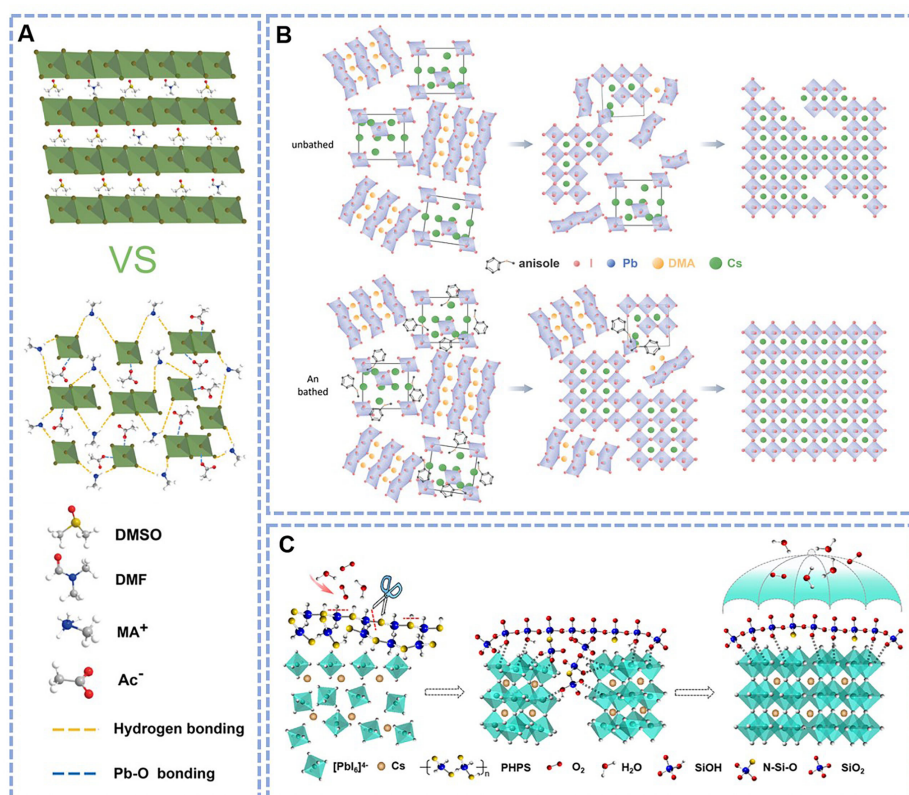
Figure 4. (A) Schematics of interaction in the precursor solutions using solvents of DMF: DMSO and MAAc, respectively. Copyright from Ref[40]. (B) Schematic illustration of the crystallization process for unbathed and anisole-bathed CsPbI$_3$ perovskite films in ambient air. Copyright from Ref[62]. (C) Schematics of PHPS-containing anti-solvent treated CsPbI$_3$ perovskite crystal growth when processing in ambient air. Copyright from Ref[42].

Jiang *et al.* used ultra-low dose transmission electron microscopy to identify the structure of DMA$^+$-incorporated CsPbI$_3$ perovskites[72]. Interestingly, they found that Cs$^+$ can be substituted by the larger organic cation DMA$^+$ to form tetragonal β-(DMA, Cs)PbI$_3$, which shows better optoelectronic properties than inorganic orthorhombic γ-phase CsPbI$_3$ [Figure 5C]. Although the devices were fabricated in a N$_2$ glove box, the air humidity stability was tested and the tetragonal β-(DMA, Cs)PbI$_3$ PSC shows an extended storage lifetime than that of orthorhombic γ-CsPbI$_3$ devices.

Based on the DMA-assisted route, Chang *et al.* introduced a multifunctional molecular additive Zn(C$_6$F$_5$)$_2$ to obtain printable CsPbI$_3$ films in ambient conditions [Figure 6A]. During printing, the contradiction between air-flow-assisted fast drying and low-quality film is reconciled, reducing trap density and improving energy level alignment[45]. Mali *et al.* fabricated β-CsPbI$_3$ with additive Zn(C$_6$F$_5$)$_2$ in ambient air with RH of 25%-30% and constructed a phase-heterojunction with γ-CsPbI$_3$, therefore producing a 21.59% PCE for a small area-device (0.09 cm^2) and an 18.43% PCE for a large area-device (18.08 cm^2)[53]. Additionally, ionic liquid, with high ionic conductivity and good thermal stability[61,73,74], was used by Du *et al.* to regulate the printed thin-film growth in ambient air. It is found that grain boundaries are decreased, iodide vacancy defects are passivated, the interfacial energy barrier is reduced, and the lattice strain is relaxed with 1-ethyl-3-methylimidazolium hydrogen sulfate (EMIMHSO$_4$) [Figure 6B][66]. Resultantly, the ambient printed CsPbI$_3$ PSCs achieve a PCE of 20.01% under 1 sun illumination (100 mW cm^{-2}) and 37.24% under indoor light illumination (1,000 lux, 365 μW cm^{-2}).
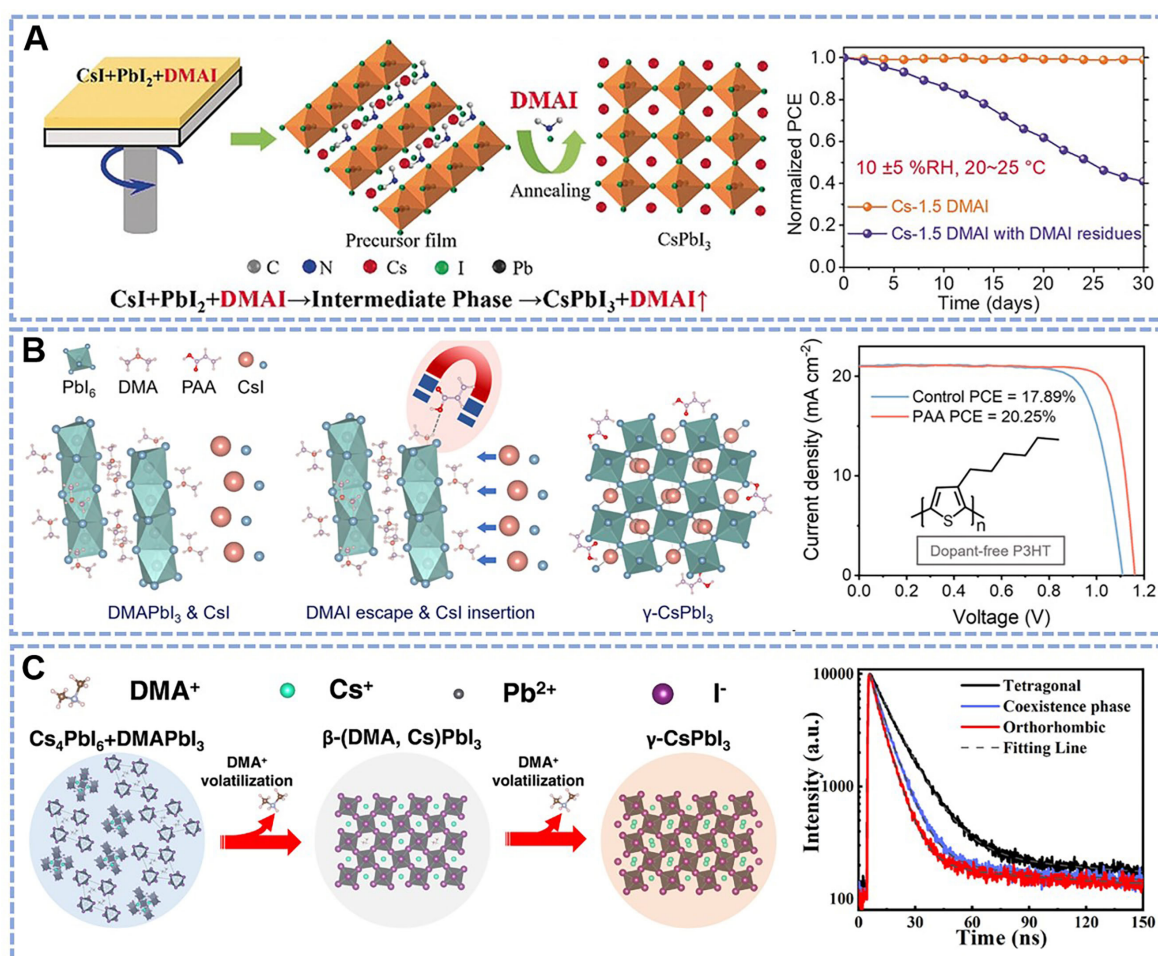
Figure 5. (A) Schematics for DMAI additive induced $CsPbI_3$ perovskite formation and the device stability based on Cs-1.5DMAI perovskite with and without DMAI residues. Copyright from Ref[44]. (B) Schematics of hydrogen bonding-assisted $CsPbI_3$ perovskite crystallization and the measured *J-V* curves of dopant-free P3HT-based $CsPbI_3$ PSCs. Copyright from Ref[21]. (C) Schematic illustration of DMAI-assisted $CsPbI_3$ perovskite formation and time-resolved photoluminescence decay spectra of tetragonal, coexistence phase and orthorhombic perovskite films. Copyright from Ref[72].

Regulating both the nucleation and crystal growth kinetics is also widely reported to realize high-quality and stable all-inorganic perovskite films under ambient conditions[48,50]. Yang *et al.* introduced imidazole halide (IMX: IMI and IMBr) into $CsPbI_2Br$ perovskite, which can form a low-dimensional intermediate phase to help improve the film quality in ambient air [Figure 6C][48].

Besides, by introducing effective additives, Pb-related defects could be passivated, further improving the PCE and stability of PSCs. Wang *et al.* prepared $CsPbI_3$ perovskite films by introducing an additive 1,2-di(thiophen-2-yl)ethane-1,2-dione (DED) to form a chelate for effectively passivating Pb-related defects and suppressin ion migration, thus boosting a PCE to 21.15%[52].

Considering the negative effect of moisture on the performance of $CsPbX_3$ PSCs, constructing a hydrophobic layer to protect perovskite films from water invasion is an effective way to improve the stability[46,47,49]. For instance, Fu *et al.* introduced 3,5-difluorobenzoic acid hydrazide (FBJ), which features a stronger absorbance on $CsPbI_3$ than water, to regulate traps and prevent external erosions, thus realizing a
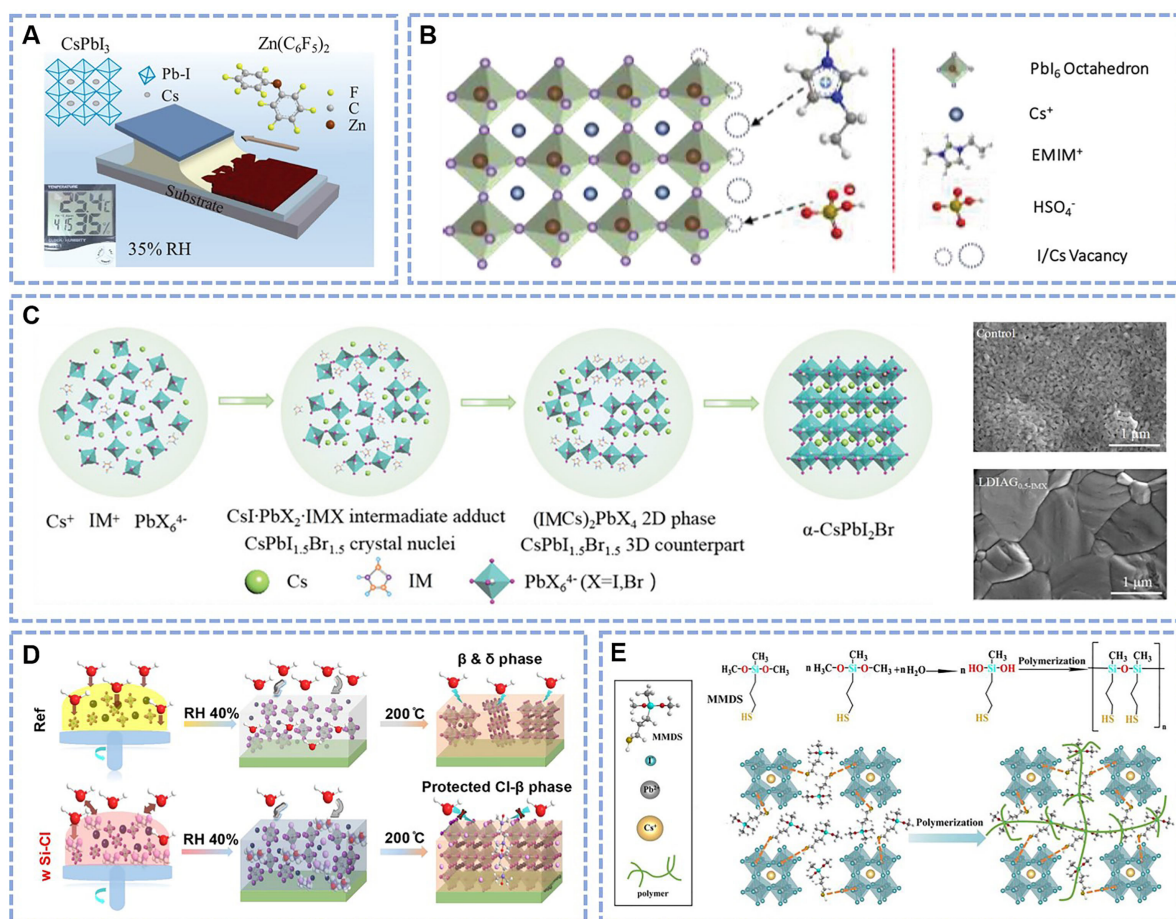
Figure 6. (A) Schematics of printed CsPbI$_3$ films modified by Zn(C$_6$F$_5$)$_2$. Copyright from Ref[45]. (B) Schematic illustration of defect passivation for CsPbI$_3$ perovskites enabled by EMIMHSO$_4$. Copyright from Ref[66]. (C) Schematic diagram of CsPbI$_2$Br perovskite crystallization process via low-dimensional intermediate-assisted growth strategy and top-view scanning electron microscope images of the control and optimized perovskite films. Copyright from Ref[48]. (D) Schematics of the chlorination and solid protection of the perovskites with humidity-assisted strategy via Si-Cl. Copyright from Ref[47]. (E) Schematic illustration of CsPbI$_3$ perovskite formation via humidity-assisted polymerization strategy by MMDS. Copyright from Ref[51].

high V_{oc} of 1.225 V for inverted CsPbI$_3$ devices[49]. Differently, humidity-assisted strategy based on hydrolysis reaction to consume water has been developed by the same group in recent years. Moisture-sensitive 1,2-bis(chlorodimethylsilyl)ethane (Si-Cl) molecules were reported to rapidly react with ambient moisture to reduce erosion during coating of perovskite films in air conditions [Figure 6D][47]. The hydrolysis products of hydrogen chloride (HCl) can chlorinate CsPbI$_3$, and the spontaneous polymerization of 1,2-bis(hydroxydimethylsilyl)ethane (Si-OH) could fill the grain boundaries for solid protection, which could regulate grain growth for better crystallization and enhanced the stability of CsPbI$_3$. In addition, maleic anhydride (MAAD) works similarly due to hydrolysis to stabilize CsPbI$_3$ films prepared with a wide humidity operating window. The hydrolysis product of maleic acid (MAAC) contains two carboxylic groups, which have strong Lewis acid-based interaction with CsPbI$_3$, thus improving the crystallization, trap passivation, and phase stability[46]. Apart from hydrolysis reaction, a humidity-assisted polymerizable additive was also used to improve the film stability and passivate defects by coordinating with Pb^{2+} [Figure 6E]. It is reported that mercaptopropylme-methyldimethoxysilane (MMDS) can react with water and form polymers in humid air[51]. Its existence at grain boundaries could not only prevent moisture invasion but also passivate under-coordinated Pb^{2+} via the interaction with the -SH group. Therefore,

regardless of fabrication in relatively high humidity (40%~80%), a PCE of 19% can be obtained for $CsPbI_3$ PSCs, in association with enhanced operational stability.
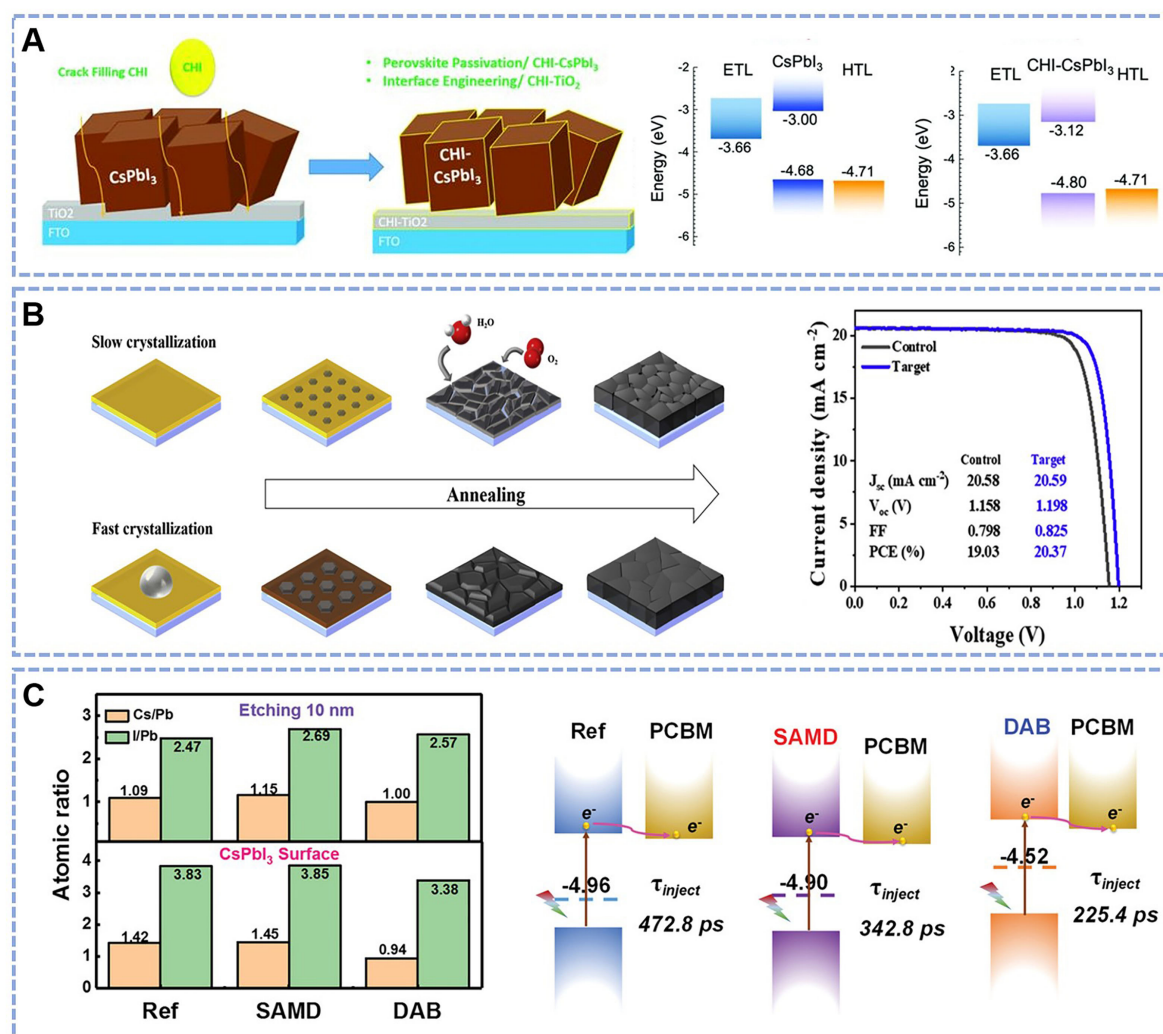
Interface engineering

Interfaces between perovskites and charge transport layers play an important role in PSCs with high PCE and stability since charge carriers need to be extracted and the moisture invasion generally happens from the surface. Thereby, modifying the interface is regarded as an effective approach to reducing defects, improving the energy alignment, increasing the charge extraction rate, enhancing the stability, *etc.*, which render the high-performance air-processed inorganic PSCs[61,63].

Wang *et al.* fabricated thermodynamically stabilized β-$CsPbI_3$ and developed a crack-filling modification strategy to improve the PCE of air-processed PSCs via surface treatment with choline iodide (CHI) [Figure 7A][60]. It is indicated that CHI can go through the pinholes and cracks and then penetrate into the bulk $CsPbI_3$ films. As a result, the traps are greatly passivated and the energy-level alignments at both the upper and bottom interfaces are improved, thus boosting the PCE to 18%. Chen *et al.* utilized 18-crown-6 ether (Crown) to stabilize/passivate α-$CsPbI_3$ fabricated in dry air with RH of 10%-15%[54]. The strong interaction between Crown and Cs^+ on the surface not only reduces humidity sensitivity but also concurrently passivates surface defects and reduces related migrations. Therefore, an efficiency of 16.9% is achieved for small-area devices (0.1 cm^2) and 11.8% for large-area modules (16 cm^2).

Additionally, the morphology and crystal structure of $CsPbX_3$ films can be regulated by intermediate treatment before annealing. Yoon *et al.* dropped the solution of methyl ammonium chloride (MACl) successively to control the intermediate state of the crystallization process of $CsPbI_3$ perovskites deposited in ambient air (RH: 15%-30%) [Figure 7B][55]. It is concluded that the crystallization process is accelerated, leading to a uniform and dense film with few pinholes. Together with the post-surface passivation with octyl ammonium iodide, the efficiency of PSCs is improved to 20.37%. Recently, Li *et al.* comparatively investigated the influence of intermediate- and post-treatment on the PCE of air-prepared inverted $CsPbI_3$ PSCs[57]. Using formamidinium (FA) salts for intermediate treatment, crystallization rate is accelerated, and the shortened exposure time is found beneficial for water resistance. Compared to the post-treatment method, the films finely tuned by intermediate treatment show pinhole-free morphology with reduced defects and better energy level alignment, significantly enhancing PCE and stability.

In addition to molecular passivation at the film surface, Fu *et al.* reported that the 1,4-butanediamine (DAB) modification could polish the intrinsically formed lead-poor surface and eliminate the nonstoichiometric components [Figure 7C][56]. Therefore, the deep-energy-level p-type traps are reduced, improving charge transfer at the $CsPbI_3$/PCBM interface. This polishing treatment promotes the efficiency to 19.84% and improves the operational stability to 1,000 h. Recently, Guo *et al.* introduced N,N'-diphenylthiourea (DPhTA) to construct a gradual $CsPbI_3$/PbS heterojunction at the top of $CsPbI_3$ surface, thus resulting in a V_{oc} of 1.20 V and a PCE over 20%[58].

Besides, Qiu *et al.* proposed a strategy via dipolar chemical bridge (DCB) to facilitate the charge transport at the perovskite/TiO_2 interface[59]. By employing 4-aminobutyric acid (CA) and 3-amino-1-propanesulfonic acid (SA) at the buried interface, the interfacial energy loss is dramatically reduced and the crystallinity of perovskites in air (RH = 30%) is improved. Therefore, the optimized $CsPbI_3$ PSCs achieve a PCE of 21.86 % with a high V_{oc} of 1.26 V.

Figure 7. (A) Schematics of crack-filling interface engineering and the energy diagram of the CsPbI$_3$ layers. Copyright from Ref[60].(B) Schematic diagram of perovskite crystallization process before and after methyl ammonium chloride treatment and the J-V curves. Copyright from Ref[55].(C) X-ray photoelectron spectroscopy results at the surface and 10 nm depth and schematic diagram of the electron-transport dynamics based on the reference and polished films. Copyright from Ref[56].

CONCLUSION AND OUTLOOK

All-inorganic CsPbX$_3$ perovskites, with Cs$^+$ completely substituting organic components, possess remarkably improved thermal and light stability compared to their organic-inorganic hybrid counterparts. Despite tremendous attention given to the all-inorganic PSCs, most of the fabrication is conducted in a glovebox with an inert atmosphere, which is unfavorable for future large-scale production and commercialization. Fabricating CsPbX$_3$ in ambient air would help realize cost-effective PSCs to further boost the practical applications. However, the intrinsic crystal structural instability and the deterioration by ambient air of inorganic perovskite pose huge challenges to obtaining high-quality perovskite films with high crystallinity, low defect density and stable structure. In this review, the instability origin is analyzed from both the intrinsic characteristics and external atmosphere. On this basis, the strategies for improving the quality of all-inorganic perovskite films to achieve efficient and stable photovoltaic devices under ambient conditions are summarized.

Despite great progress in recent years, the PCE and stability of inorganic PSCs remain far from satisfactory and severe issues persist to be solved. For example, as the film properties and resultant device performance are significantly influenced by the ambient moisture, it is still challenging to widen the operating humidity window, which may complicate the operation procedure and consequently increase the fabrication costs. Therefore, more effective pathways are expected to optimize the optoelectronic properties and stability of $CsPbX_3$ perovskite films under ambient conditions with high humidity. For instance, multifunctional agents, which can effectively modulate the crystallization process and simultaneously passivate the defects of air-processed $CsPbX_3$ are required to be extensively explored. The property of water resistance still needs to be improved by developing more effective hydrophobic agents or through water-induced cross-linking strategy to consume water, especially at the film surface and grain boundaries. To further enhance the long-term stability of devices, applying dopant-free hole transport layers in regular devices is also essential. Apart from innovative techniques or agents for optimizing the $CsPbX_3$ perovskite film quality and device performance, understanding the individual effects of moisture and oxygen deeply and systematically is crucial for further enhancing the PCE and stability of the PSCs. For example, advanced characterizations, such as in-situ Grazing Incidence Wide Angle X-ray Scattering (GIWAXS) and *in-situ* photoluminescence (PL) during film formation, together with operando studies on solar cells, *etc.*, help understand the formation and degradation mechanisms under different environmental humidity or gas atmosphere. With great efforts, we believe the photovoltaic performance of $CsPbX_3$ PSCs fabricated in ambient air will be significantly promoted, which will pave the way for low-cost production of efficient and stable PSCs.

DECLARATIONS

Authors' contributions
Contribute equally to this work: Cao L, Tong Y
Investigation and original drafting: Cao L
Conceptualization and re-writing: Wang K
Revision: Tong Y
Discussing and commentary: Cao L, Tong Y, Wang K, Wang H
Supervision: Tong Y, Wang H, Wang K

Availability of data and materials
Not applicable.

Conflicts of interest
All authors declared that there are no conflicts of interest.

Ethical approval and consent to participate
Not applicable.

Consent for publication
Not applicable.

Copyright

© The Author(s) 2024.

REFERENCES

1. Green MA, Ho-baillie A, Snaith HJ. The emergence of perovskite solar cells. *Nat Photon* 2014;8:506-14. DOI

2. National Renewable Energy Laboratory. Best research-cell efficiency chart. Available from: https://www.nrel.gov/pv/cell-efficiency.html [Last accessed on 27 May 2024].

3. Park N, Grätzel M, Miyasaka T, Zhu K, Emery K. Towards stable and commercially available perovskite solar cells. *Nat Energy* 2016;1:16152. DOI

4. Boyd CC, Cheacharoen R, Leijtens T, McGehee MD. Understanding degradation mechanisms and improving stability of perovskite photovoltaics. *Chem Rev* 2019;119:3418-51. DOI PubMed

5. Tian J, Xue Q, Yao Q, Li N, Brabec CJ, Yip H. Inorganic halide perovskite solar cells: progress and challenges. *Adv Energy Mater* 2020;10:2000183. DOI

6. Kye YH, Yu CJ, Jong UG, Chen Y, Walsh A. Critical role of water in defect aggregation and chemical degradation of perovskite solar cells. *J Phys Chem Lett* 2018;9:2196-201. DOI

7. Wang K, Tong Y, Cao L, et al. Progress of inverted inorganic cesium lead halide perovskite solar cells. *Cell Rep Phys Sci* 2023;4:101726. DOI

8. Eperon GE, Paternò GM, Sutton RJ, et al. Inorganic caesium lead iodide perovskite solar cells. *J Mater Chem A* 2015;3:19688-95. DOI

9. Swarnkar A, Marshall AR, Sanehira EM, et al. Quantum dot-induced phase stabilization of α-CsPbI$_3$ perovskite for high-efficiency photovoltaics. *Science* 2016;354:92-5. DOI

10. Wang Z, Tian Q, Zhang H, et al. Managing multiple halide-related defects for efficient and stable inorganic perovskite solar cells. *Angew Chem Int Ed* 2023;62:e202305815. DOI

11. Yan L, Huang H, Cui P, et al. Fabrication of perovskite solar cells in ambient air by blocking perovskite hydration with guanabenz acetate salt. *Nat Energy* 2023;8:1158-67. DOI

12. Zhang J, Hodes G, Jin Z, Liu SF. All-inorganic CsPbX$_3$ perovskite solar cells: progress and prospects. *Angew Chem Int Ed* 2019;58:15596-618. DOI

13. Steele JA, Jin H, Dovgaliuk I, et al. Thermal unequilibrium of strained black CsPbI$_3$ thin films. *Science* 2019;365:679-84. DOI

14. Huang Y, Yin W, He Y. Intrinsic point defects in inorganic cesium lead iodide perovskite CsPbI$_3$. *J Phys Chem C* 2018;122:1345-50. DOI

15. deQuilettes DW, Vorpahl SM, Stranks SD, et al. Solar cells. Impact of microstructure on local carrier lifetime in perovskite solar cells. *Science* 2015;348:683-6. DOI

16. Shao S, Abdu-aguye M, Sherkar TS, et al. The effect of the microstructure on trap-assisted recombination and light soaking phenomenon in hybrid perovskite solar cells. *Adv Funct Mater* 2016;26:8094-102. DOI

17. Cappel UB, Svanström S, Lanzilotto V, et al. Partially reversible photoinduced chemical changes in a mixed-ion perovskite material for solar cells. *ACS Appl Mater Interfaces* 2017;9:34970-8. DOI PubMed PMC

18. Bella F, Griffini G, Correa-Baena JP, et al. Improving efficiency and stability of perovskite solar cells with photocurable fluoropolymers. *Science* 2016;354:203-6. DOI

19. Lin J, Lai M, Dou L, et al. Thermochromic halide perovskite solar cells. *Nat Mater* 2018;17:261-7. DOI

20. Liang L, Li Z, Zhou F, et al. The humidity-insensitive fabrication of efficient CsPbI$_3$ solar cells in ambient air. *J Mater Chem A* 2019;7:26776-84. DOI

21. Li M, Wang S, Ma X, et al. Hydrogen-bonding-facilitated dimethylammonium extraction for stable and efficient CsPbI$_3$ solar cells with environmentally benign processing. *Joule* 2023;7:2595-608. DOI

22. Mali SS, Patil JV, Steele JA, Rondiya SR, Dzade NY, Hong CK. Implementing dopant-free hole-transporting layers and metal-incorporated CsPbI$_2$Br for stable all-inorganic perovskite solar cells. *ACS Energy Lett* 2021;6:778-88. DOI PubMed PMC

23. Zhang X, Bai X, Wu H, et al. Water-assisted size and shape control of CsPbBr$_3$ perovskite nanocrystals. *Angew Chem Int Ed* 2018;57:3337-42. DOI

24. Aristidou N, Sanchez-Molina I, Chotchuangchutchaval T, et al. The role of oxygen in the degradation of methylammonium lead trihalide perovskite photoactive layers. *Angew Chem Int Ed* 2015;54:8208-12. DOI

25. Aristidou N, Eames C, Sanchez-Molina I, et al. Fast oxygen diffusion and iodide defects mediate oxygen-induced degradation of perovskite solar cells. *Nat Commun* 2017;8:15218. DOI PubMed PMC

26. Tsvetkov DS, Mazurin MO, Sereda VV, Ivanov IL, Malyshkin DA, Zuev AY. Formation thermodynamics, stability, and decomposition pathways of CsPbX$_3$ (X = Cl, Br, I) photovoltaic materials. *J Phys Chem C* 2020;124:4252-60. DOI

27. Liu SC, Li Z, Yang Y, et al. Investigation of oxygen passivation for high-performance all-inorganic perovskite solar cells. *J Am Chem Soc* 2019;141:18075-82. DOI

28. Liang J, Zhao P, Wang C, et al. CsPb$_{0.9}$Sn$_{0.1}$IBr$_2$ based all-inorganic perovskite solar cells with exceptional efficiency and stability. *J Am Chem Soc* 2017;139:14009-12. DOI

29. Jena AK, Kulkarni A, Sanehira Y, Ikegami M, Miyasaka T. Stabilization of α-CsPbI$_3$ in ambient room temperature conditions by

incorporating Eu into CsPbI$_3$. *Chem Mater* 2018;30:6668-74. DOI

30.   Yang F, Hirotani D, Kapil G, et al. All-inorganic CsPb$_{1-x}$Ge$_x$I$_2$Br perovskite with enhanced phase stability and photovoltaic performance. *Angew Chem Int Ed* 2018;57:12745-9. DOI

31.   Mali SS, Patil JV, Hong CK. Hot-air-assisted fully air-processed barium incorporated CsPbI$_2$Br perovskite thin films for highly efficient and stable all-inorganic perovskite solar cells. *Nano Lett* 2019;19:6213-20. DOI PubMed

32.   Patil JV, Mali SS, Hong CK. A-site rubidium cation-incorporated CsPbI$_2$Br all-inorganic perovskite solar cells exceeding 17% efficiency. *Solar RRL* 2020;4:2000164. DOI

33.   Chen S, Zhang T, Liu X, et al. Lattice reconstruction of La-incorporated CsPbI$_2$Br with suppressed phase transition for air-processed all-inorganic perovskite solar cells. *J Mater Chem C* 2020;8:3351-8. DOI

34.   Patil JV, Mali SS, Park DW, Hong CK. Novel ytterbium-doped CsPbI$_2$Br thin-films-based inorganic perovskite solar cells toward improved phase stability. *Mater Today Chem* 2021;22:100557. DOI

35.   Mali SS, Patil JV, Shinde PS, de Miguel G, Hong CK. Fully air-processed dynamic hot-air-assisted M:CsPbI$_2$Br (M: Eu^{2+}, In^{3+}) for stable inorganic perovskite solar cells. *Matter* 2021;4:635-53. DOI

36.   Patil JV, Mali SS, Hong CK. Holmium rare earth metal ion incorporated and ambient-air processed all-inorganic γ-CsPbI$_{2.5}$Br$_{0.5}$ perovskite solar cells yielding high efficiency and stable performance. *J Mater Chem A* 2023;11:21312-21. DOI

37.   Xiang S, Fu Z, Li W, et al. Highly air-stable carbon-based α-CsPbI$_3$ perovskite solar cells with a broadened optical spectrum. *ACS Energy Lett* 2018;3:1824-31. DOI

38.   Duan C, Cui J, Zhang M, et al. Precursor engineering for ambient-compatible antisolvent-free fabrication of high-efficiency CsPbI$_2$Br perovskite solar cells. *Adv Energy Mater* 2020;10:2000691. DOI

39.   Yue Y, Yang R, Zhang W, Cheng Q, Zhou H, Zhang Y. Cesium cyclopropane acid-aided crystal growth enables efficient inorganic perovskite solar cells with a high moisture tolerance. *Angew Chem Int Ed* 2024;63:e202315717. DOI

40.   Wang X, Ran X, Liu X, et al. Tailoring component interaction for air-processed efficient and stable all-inorganic perovskite photovoltaic. *Angew Chem Int Ed* 2020;59:13354-61. DOI

41.   Saparbaev A, Zhang M, Kuvondikov V, et al. High-performance CsPbI$_3$ perovskite solar cells without additives in air condition. *Solar Energy* 2021;228:405-12. DOI

42.   Wang T, Yang Q, Chen Y, et al. Stitching perovskite grains with perhydropoly(Silazane) anti-template-agent for high-efficiency and stable solar cells fabricated in ambient air. *Energy Environ Mater* 2023;6:e12554. DOI

43.   Luo P, Xia W, Zhou S, et al. Solvent engineering for ambient-air-processed, phase-stable CsPbI$_3$ in perovskite solar cells. *J Phys Chem Lett* 2016;7:3603-8. DOI

44.   Wang Y, Liu X, Zhang T, et al. The role of dimethylammonium iodide in CsPbI$_3$ perovskite fabrication: additive or dopant? *Angew Chem Int Ed* 2019;58:16691-6. DOI

45.   Chang X, Fang J, Fan Y, et al. Printable CsPbI$_3$ perovskite solar cells with PCE of 19% via an additive strategy. *Adv Mater* 2020;32:e2001243. DOI

46.   Fu S, Li X, Wan J, Zhang W, Song W, Fang J. In situ stabilized CsPbI$_3$ for air-fabricated inverted inorganic perovskite photovoltaics with wide humidity operating window. *Adv Funct Mater* 2022;32:2111116. DOI

47.   Fu S, Zhang W, Li X, Guan J, Song W, Fang J. Humidity-assisted chlorination with solid protection strategy for efficient air-fabricated inverted CsPbI$_3$ perovskite solar cells. *ACS Energy Lett* 2021;6:3661-8. DOI

48.   Yang S, Wen J, Liu Z, et al. A key 2D intermediate phase for stable high-efficiency CsPbI$_2$Br perovskite solar cells. *Adv Energy Mater* 2022;12:2103019. DOI

49.   Fu S, Sun N, Le J, et al. Tailoring defects regulation in air-fabricated CsPbI$_3$ for efficient inverted all-inorganic perovskite solar cells with V$_{oc}$ of 1.225 V. *ACS Appl Mater Interfaces* 2022;14:30937-45. DOI

50.   Xu S, Kang C, Huang Z, et al. Dual-functional quantum dot seeding growth of high-quality air-processed CsPbI$_2$Br film for carbon-based perovskite solar cells. *Solar RRL* 2022;6:2100989. DOI

51.   Lu C, Li X, Guo X, et al. Efficient inverted CsPbI3 perovskite solar cells fabricated in common air. *Chem Eng J* 2023;452:139495. DOI

52.   Wang J, Che Y, Duan Y et al. 21.15%-efficiency and stable γ -CsPbI$_3$ perovskite solar cells enabled by an acyloin ligand. *Adv Mater* 2023;35:2210223. DOI

53.   Mali SS, Patil JV, Shao J, et al. Phase-heterojunction all-inorganic perovskite solar cells surpassing 21.5% efficiency. *Nat Energy* 2023;8:989-1001. DOI

54.   Chen R, Hui Y, Wu B, et al. Moisture-tolerant and high-quality α-CsPbI$_3$ films for efficient and stable perovskite solar modules. *J Mater Chem A* 2020;8:9597-606. DOI

55.   Yoon SM, Min H, Kim JB, Kim G, Lee KS, Seok SI. Surface engineering of ambient-air-processed cesium lead triiodide layers for efficient solar cells. *Joule* 2021;5:183-96. DOI

56.   Fu S, Le J, Guo X, et al. Polishing the lead-poor surface for efficient inverted CsPbI$_3$ perovskite solar cells. *Adv Mater* 2022;34:e2205066. DOI

57.   Li T, Li W, Wang K, et al. Interface engineering with formamidinium salts for improving ambient-processed inverted CsPbI$_3$ photovoltaic performance: intermediate- vs post-treatment. *ACS Appl Mater Interfaces* 2023;15:51350-9. DOI

58.   Guo X, Lu C, Zhang W, et al. In situ surface sulfidation of CsPbI$_3$ for inverted perovskite solar cells. *ACS Energy Lett* 2024;9:329-35. DOI

59. Qiu J, Mei X, Zhang M, et al. Dipolar chemical bridge induced CsPbI$_3$ perovskite solar cells with 21.86 % efficiency. *Angew Chem Int Ed* 2024;63:e202401751. DOI

60. Wang Y, Dar MI, Ono LK, et al. Thermodynamically stabilized β-CsPbI$_3$-based perovskite solar cells with efficiencies >18%. *Science* 2019;365:591-5. DOI

61. Wang K, Su Z, Chen Y, et al. Dual bulk and interface engineering with ionic liquid for enhanced performance of ambient-processed inverted CsPbI$_3$ perovskite solar cells. *J Mater Sci Technol* 2022;114:165-71. DOI

62. Jeong W, Jang G, Ma S, et al. Unraveling the antisolvent bathing effect on CsPbI$_3$ crystallization under ambient conditions. *Adv Funct Mater* 2022;32:2207342. DOI

63. Mali SS, Patil JV, Rondiya SR, et al. Terbium-doped and dual-passivated γ-CsPb(I$_{1-x}$Br$_x$)$_3$ inorganic perovskite solar cells with improved air thermal stability and high efficiency. *Adv Mater* 2022;34:e2203204. DOI

64. Rico-yuson CA, Danwittayakul S, Kumar S, Hornyak GL, Bora T. Sequential dip-coating of CsPbBr$_3$ perovskite films in ambient conditions and their photovoltaic performance. *J Mater Sci* 2022;57:10285-98. DOI

65. Wang K, Gao C, Xu Z, et al. In-situ hot oxygen cleansing and passivation for all-inorganic perovskite solar cells deposited in ambient to breakthrough 19% efficiency. *Adv Funct Mater* 2021;31:2101568. DOI

66. Du Y, Tian Q, Chang X, et al. Ionic liquid treatment for highest-efficiency ambient printed stable all-inorganic CsPbI$_3$ perovskite solar cells. *Adv Mater* 2022;34:e2106750. DOI

67. Dong C, Han X, Zhao Y, Li J, Chang L, Zhao W. A green anti-solvent process for high performance carbon-based CsPbI$_2$Br all-inorganic perovskite solar cell. *Solar RRL* 2018;2:1800139. DOI

68. Wang Y, Wu J, Zhang P, et al. Stitching triple cation perovskite by a mixed anti-solvent process for high performance perovskite solar cells. *Nano Energy* 2017;39:616-25. DOI

69. Xu W, Ji R, Liu P, et al. In situ-fabricated perovskite nanocrystals for deep-blue light-emitting diodes. *J Phys Chem Lett* 2020;11:10348-53. DOI

70. Zhang F, Zhu K. Additive engineering for efficient and stable perovskite solar cells. *Adv Energy Mater* 2020;10:1902579. DOI

71. Patil JV, Mali SS, Hong CK. Reducing defects of all-inorganic γ-CsPbI$_2$Br thin films by ethylammonium bromide additives for efficient perovskite solar cells. *ACS Appl Mater Interfaces* 2022;14:25576-83. DOI PubMed

72. Jiang Y, Xu T, Du H, et al. Organic-inorganic hybrid nature enables efficient and stable CsPbI$_3$-based perovskite solar cells. *Joule* 2023;7:2905-22. DOI

73. Bai S, Da P, Li C, et al. Planar perovskite solar cells with long-term stability using ionic liquid additives. *Nature* 2019;571:245-50. DOI

74. Yang D, Yang R, Ren X, et al. Hysteresis-suppressed high-efficiency flexible perovskite solar cells using solid-state ionic-liquids for effective electron transport. *Adv Mater* 2016;28:5206-13. DOI